Rare Metal Materials and Engineering
Volume 49, Issue 6, June 2020
Available online at www.rmme.ac.cn

Science Press

Cite this article as: Rare Metal Materials and Engineering, 2020, 49(6): 1946-1956.

ARTICLE

Deformation Behavior of TA1/AZ31B Multi-layer Composites During Isothermal Compression Processing

Zhang Bing[1,2,3], Yao Su[1,3], Wang Qiuyu[1,3], Li Juan[2], Zhang Dong[2], Zhao Tianli[1,2], Wang Wen[1,2], Cai Jun[1,2], Wang Kuaishe[1,2]

[1] Xi'an University of Architecture and Technology, Xi'an 710055, China; [2] State Key Laboratory of Nickel and Cobalt Resource Integrated Utilization, Jinchuan Group Co., Ltd, Jinchang 737100, China; [3] National & Local Engineering Researching Center for Functional Materials Processing, Xi'an 710055, China

Abstract: Isothermal compression experiments were performed to investigate the hot deformation behavior of TA1/AZ31B multi-layer composites. Flow stress-strain curves were obtained for deformation at temperatures from 573 K to 723 K within the strain rate range from 0.01 s^{-1} to 10 s^{-1}, and the height reduction range from 30% to 50%. The results show that both TA1 and AZ31B have plastic deformation during the compression bonding process. However, all layers' deformation of TA1/AZ31B multi-layer composite does not occur at the same time and is not uniform. The deformation of AZ31B is larger than that of TA1, and dynamic recrystallization of AZ31B occurs during the deformation process. When the strain rate is 10 s^{-1}, necking and fracture occurs in the middle TA1 layer. Based on the flow stress-strain curves, the Arrhenius-type constitutive equation could precisely predict the flow stress behavior of TA1/AZ31B multi-layer composite. The value of the correlation coefficient is 0.991 when the average absolute relative error is 3.976%. The processing map at true strain of 0.5 for TA1/AZ31B multi-layer composite was developed using the dynamic materials model (DMM) theory. The processing map of isothermally compressed TA1/AZ31B multi-layer composite exhibits that the optimum parameters are the temperature of 723 K and the strain rate of 0.01 s^{-1} with power dissipation's maximum efficiency of 28%. In the meanwhile, there is one instability domain in the processing map of isothermally compressed TA1/AZ31B multi-layer composite; it is in the deformation temperature range from 573 K to 692 K and the strain rate range from 0.6 s^{-1} to 10 s^{-1}.

Key words: TA1/AZ31B multi-layer composites; isothermal compression; deformation behavior; constitutive equation; processing map

During recent years, laminated metal composites (LMCs) have attached great attention due to their special properties, such as magnetic properties and complementarity among constituent metals, electrical properties, corrosion resistance and advanced mechanical performance. So far, there are various techniques that have been improved for the production of LMCs, for example, friction-stir welding, diffusion bonding, roll bonding and explosive welding. In comparison with other techniques, roll bonding has been commonly used due to its low cost and efficiency. It is a kind of solid-state welding processing where various layers of either dissimilar or similar metals have been stacked together and hence to produce multi-layer composites[1]. However, the technique of roll bonding has been influenced by rolling reduction[1-3], rolling temperature[2,3], rolling speed[4], initial thickness between dissimilar metals[2,4], rolling direction[4], surface roughness[2], and heat treatment during the roll bonding processing[3,4]. Till now, roll bonding has already been used successfully for the manufacturing of LMCs, such as Cu/Al[5, 6], Mg/Al[7] and Ti/Al[8].

TA1/AZ31B multi-layer composites possess the potential for the industrial applications because of their wonderful mechanical properties, low density, strong shock absorption performance and corrosion resistance[9-11]. However, the TA1 and AZ31B are hexagonal close-packed structure, and the

Received date: June 25, 2019
Foundation item: National Natural Science Foundation of China (51874226); State Key Laboratory of Nickel and Cobalt Resource Integrated Utilization (301170504); Xi'an Science and Technology Planning Project (201805033YD11CG17(8)); Xi'an University of Architecture & Technology (JC1507)
Corresponding author: Zhang Bing, Ph. D., Professor, College of Metallurgy Engineering, Xi'an University of Architecture and Technology, Xi'an 710055, P. R. China, Tel: 0086-29-82202931, E-mail: r.zhang1112@163.com

AZ31B melting point (923 K) is extremely different from that of TA1 (1933 K). In the range 573~673 K of deformation temperature, the deformation behaviors, mechanical properties, and flow characteristics of TA1 and AZ31B are diverse, which would lead to the inhomogeneous deformation between TA1 and AZ31B, and the cracks during roll bonding processing. Thus, there are still a few studies on the deformation behaviors of layer-wise of TA1/AZ31B multi-layer composites in roll bonding processing. Yasser et al[11] applied the Al-alloy interlayer for the bonding of the AZ31 and Ti for the manufacturing of the composites through the cold roll bonding. It has been measured that there is 44% of the threshold deformation of the rolling reduction. The results show that the growth of the heat treatment temperature would lead to the appearance of the transition layer along the Al/AZ31 interface. It has been found that there was none intermetallic compound over the interface of Ti and Al. According to Wu et al[12], explosive welding can be used to produce the TA2/AZ31B laminated composites. According to the results, there is the coexistence of the wavy and straight interfaces over the bonding area. There was obvious element diffusion when it has been heated at 723~763 K for 4 and 8 h. There was a significant increase of the hardness of AZ31B and TA2 because of plastic deformation and strain hardening. The composite plates' mechanical properties have been improved dramatically in comparison with those of the base plate AZ31B. Motevalli[13] used roll bonding to produce the Al/Ti/Mg laminated composites. The results of the first accumulative roll bonding (ARB) cycles show that Ti and Mg layers have been fractured and necked through this process because of the non-uniform distribution and strain hardening of the matrix's reinforcement layers. Through five ARB cycles, it is formed that the tri-metal Al/Ti/Mg multilayer composite has homogeneous distribution. There was an increase of the corresponding hardness.

During roll bonding processing, it is an important problem for TA1/AZ31B multi-layer composite material to effectively control the cooperation-deformation of TA1 and AZ31B. In the present work, TA1/AZ31B multi-layer composites were studied by isothermal plane compression. The deformation behaviors and microstructure of TA1/AZ31B multi-layer composites were investigated at different temperatures and strain rates by flow stress-strain curves, and constitutive equations were established. In addition the optimum processing parameters of TA1/AZ31B multi-layer composites by roll bonding were studied by processing maps and macrostructure observations.

1 Experiment

In this experiment, TA1 and AZ31B sheets after being annealed were used for isothermal plane compression. The chemical composition (wt%) of TA1 and AZ31B is given in Table 1. The optical microstructure of TA1 and AZ31B are shown in Fig.1a and 1b, respectively. The experimental specimens, with the size of TA1 of 1.0 mm (T)×15 mm (W)×45 mm (L) and AZ31B of 3.5 mm (T)×15 mm (W)×45 mm (L), were prepared by electrodischarge wire cutting. Both the ends and the plate surface of TA1 and AZ31B were treated by sandpaper and alcohol, and TA1 sheets and AZ31B sheets were then stacked into five layers according to TA1-AZ31B-TA1-AZ31B-TA1. The final size of the specimen was 10 mm (T) ×15 mm (W) ×45 mm (L). The compression experiment is shown in Fig.2. The specimens before and after compressing are presented in Fig.3.

The Gleeble-1500 machine was used for the implementation of the isothermal plane compression experiment. The compression temperatures were between 573 and 723 K, the interval of which was 50 K. The strain rates were correspondingly 0.01, 0.1, 1.0, 10 s^{-1}. All of the specimens have been heated until reaching to the desired temperature. Then, they were held for 5 min to obtain the uniform temperature distribution before compression. During the process, there was none lubrication over the top or bottom of these specimens. Afterwards, a compression deformation of the specimens to 40% of their original height was carried out hence to get a true strain around 0.5. Afterwards, air-cooling was performed to the room temperature. Fig.4 presents the thermo-deformation schedule of the plan compression. The flow stress data of every

Table 1 Chemical composition of TA1 and AZ31B (wt%)

TA1	Fe	C	Si	N	H	O	Ti
	0.15	0.05	0.1	0.03	0.015	0.15	Bal.
AZ31B	Al	Mn	Zn	Ca	Si	Cu	Mg
	2.9	0.56	1.05	0.03	0.08	0.01	Bal.

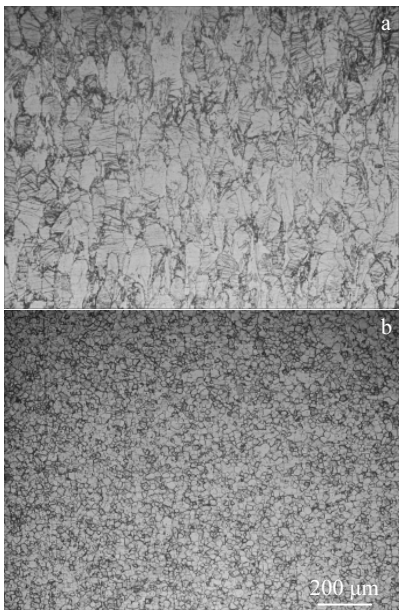

Fig.1 Microstructures of original material: (a) AZ31B and (b) TA1

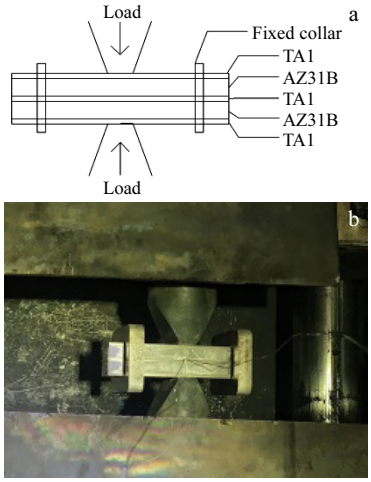

Fig.2 Compression experiment of TA1/AZ31B multi-layer composite

Fig.3 Compression specimen of TA1/AZ31B multi-layer composites: (a) before compressing and (b) after compressing

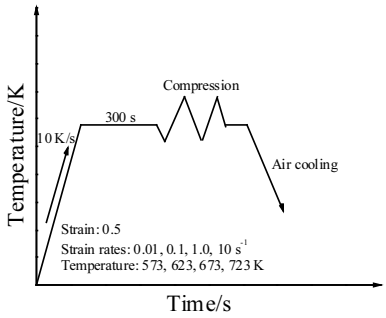

Fig.4 Thermo-deformation schedule of the compression experiment

plane compression has been recorded for the calculation of the efficiency of the energy dissipation. Afterwards, the instability parameter of the TA1/AZ31B composites' processing map was analyzed. The specimens were deformed and then sectioned along the compression axis. Metallographic specimens were prepared through the standard techniques. The solution of 15% HNO_3 and 80% H_2O were used for the etching of the AZ31B layer of TA1/AZ31B multi-layer composite. Subsequently, 4% picric acid, 4% acetic acid, 8% H_2O, and 84% ethyl alcohol were used for the etching of the TA1 layer of TA1/AZ31B multi-layer composite. The OLYMPUS GX51 optical microscope was used for the microstructure observations.

2 Results and Discussion

2.1 Flow stress-strain curves of TA1 and AZ31B

Fig.5 illustrates the flow stress-strain curves of AZ31B in the temperature range of 573~723 K with various strain rates. Fig.5 demonstrates that when the true strain is less than 0.1, the flow stress quickly increases with increasing the strain. It is because the dislocation density increases rapidly at initial deformation stages. The interlaced dislocations structures impede the movement of dislocation, leading to the increase in flow stress, which makes the deformation of AZ31B exhibit work-hardening. The flow stress decreases after reaching the peak stress with increasing the strain. When the true strain exceeds 0.4, the flow stress continuously maintains a steady status implying the occurrence of dynamic recovery and dynamic recrystallization (DRX). It is because the dislocations have sufficient time to activate the higher capability of climbing and sliding, leading to softening behavior such as DRX and DRV, thus reducing the density of dislocations resulting in the decrease of work-hardening. Therefore, work-hardening phenomena disappear gradually until both of the softening and work- hardening phenomena acquire a steady state[14]. When the strain rate is 10 s^{-1} (Fig.5d), the curves show significant serrate oscillation, which is the result of dynamic recrystallization competing with work-hardening, alternate hardening and softening implying that discontinuous dynamic recrystallization (DDRX) with the occurrence of flow instability.

Fig.6 illustrates the flow stress-strain curves of TA1 in the temperature range of 573~723 K with various strain rates. It can be found from Fig.6 that the flow stress increases rapidly when the true strain is less than 0.05. Then, the flow stress shows a slowly increase tendency with increasing the true strain. The reason is that the deformation of TA1 in the temperature range of 573~723 K belongs to cold deformation process and the rate of dislocation generating increases rapidly. Therefore, work-hardening is obvious, leading to the increasing of deformation resistance of material. At the same strain rate, the flow stress decreases with increasing the temperature, suggesting that thermal activation and the kinetic energy between atoms increase, the activity of vacancy and dislocation increases, so the flow stress decreases. When the strain rates are 1.0 and 10 s^{-1} (Fig.6c, 6d), the flow stress-strain curves reach the peak stress at strain of 0.3. Then, the curves of stress have a slight decline with the increase of true strain. This flowing behavior is ascribed to the co-existence of work hardening and softening

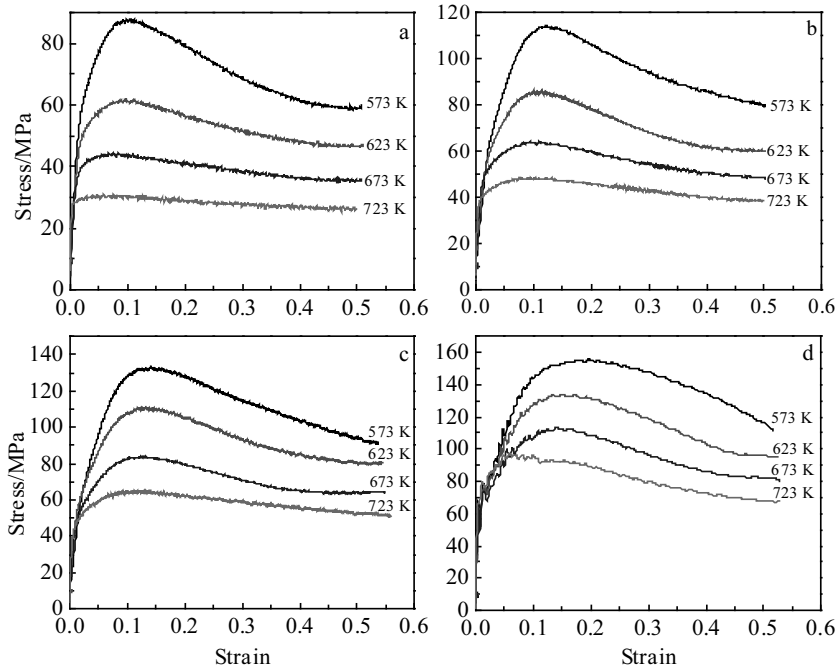

Fig.5 Flow stress-strain curves of AZ31B at different strains rates: (a) $\dot{\varepsilon}$ =0.01 s^{-1}, (b) $\dot{\varepsilon}$ =0.1 s^{-1}, (c) $\dot{\varepsilon}$ =1.0 s^{-1}, and (d) $\dot{\varepsilon}$ =10 s^{-1} for various temperatures

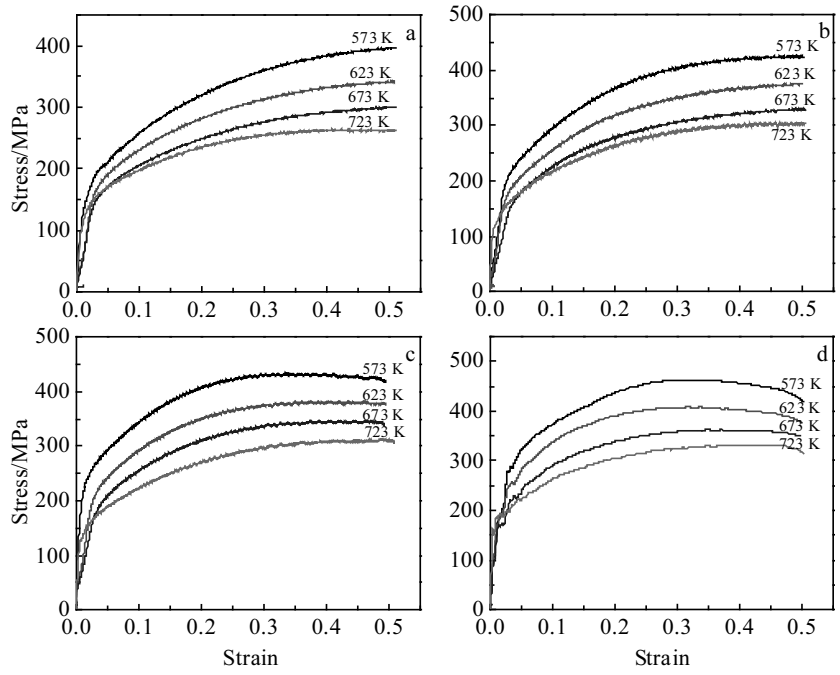

Fig.6 Flow stress-strain curves of TA1 at different strains rates: (a) $\dot{\varepsilon}$ =0.01 s^{-1}, (b) $\dot{\varepsilon}$ =0.1 s^{-1}, (c) $\dot{\varepsilon}$ =1.0 s^{-1}, and (d) $\dot{\varepsilon}$ =10 s^{-1} for various temperatures

such as the dynamic recovery (DRV) and dynamic recrystallization (DRX).

2.2 Flow stress-strain curves of TA1/AZ31B multi-layer composite

Fig.7 illustrates the flow stress-strain curves of TA1/AZ31B multi-layer composites in the temperature range of 573~723 K with various strain rates. It shows that the flow stress of TA1/AZ31B multi-layer composites decreases with the increasing of deformation temperature at the same strain rate. At the same deformation temperature, the flow stress increases with

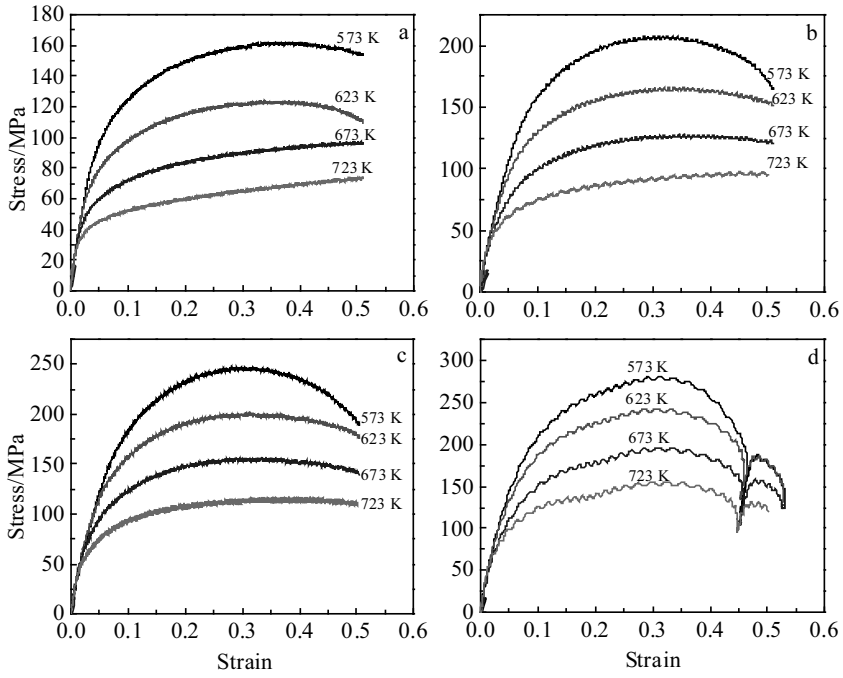

Fig.7 Flow stress-strain curves of TA1/AZ31B multi-layer composite at different strains rates: (a) $\dot{\varepsilon}$ =0.01 s^{-1}, (b) $\dot{\varepsilon}$ =0.1 s^{-1}, (c) $\dot{\varepsilon}$ =1.0 s^{-1}, and (d) $\dot{\varepsilon}$ =10 s^{-1} for various temperatures

the increasing of deformation rate, and this can also be observed in Fig.8. It indicates that the TA1/AZ31B multi-layer composite has positive strain rate sensitivity under this experiment condition, i.e. the larger the strain rate, the lower the deformation temperature; it is more difficult for the TA1/AZ31B multi-layer composite to achieve steady deformation. During the compressed composite process, dynamic recrystallization (DRX) occurs in AZ31B of the composites. When the deformation temperature increases from 573 K to 723 K，the average peak stress of TA1/AZ31B multi-layer composite decreases by 113 MPa (Table 2).

According to previous studies, the temperature of dynamic recrystallization of AZ31B is above 523 K under this experiment condition. Therefore, the flow stress exhibits obvious work-hardening before reaching the peak stress and then the stress decreases, when the temperature is in range of 573~723 K. With increasing the strain rate (from 0.01 s^{-1} to 10 s^{-1}), the flow stress increases. The curves show significant serrate oscillation, which is the result of dynamic recrystallization competing with work-hardening, alternate hardening and softening between TA1 and AZ31B, implying that discontinuous deformation with flow instability has occurred. When

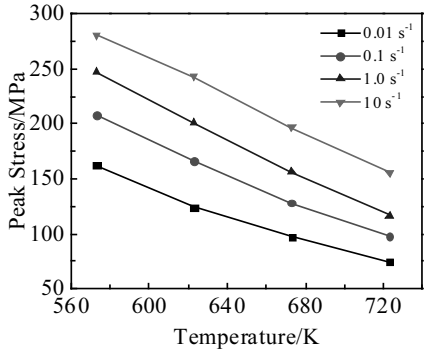

Fig.8 Relationship between peak stress, deformation temperatures and strain rates

Table 2 Peak stress value of TA1, AZ31B and TA1/AZ31B multi-layer composites (MPa)

	Temperature/K	0.01 s^{-1}	0.1 s^{-1}	1.0 s^{-1}	10 s^{-1}
TA1	573	398.04	311.61	433.56	463.5
	623	341.51	262.63	378.12	408.22
	673	299.35	220.87	336.69	359.68
	723	263.17	207.92	301.83	323.66
	Difference	134.87	103.69	131.73	139.84
AZ31B	573	88.134	114.19	132.88	126.57
	623	61.587	85.835	110.54	113.76
	673	43.95	63.886	83.663	96.539
	723	30.171	47.941	63.92	95.271
	Difference	57.963	66.249	68.96	31.299
TA1/AZ31B	573	162.45	208.11	247.06	280.92
	623	124.1	166.31	201.12	242.86
	673	97.388	128.27	156.3	196.54
	723	74.263	97.734	116.46	155.77
	Difference	88.187	110.376	130.6	125.15

the deformation temperature increases, the flow stress decreases, and the stress tends to be a relatively stable state.

More obviously, from Fig.7d, when the strain rate is 10 s^{-1}, the stress drops sharply after reaching the peak stress. When the true strain reaches 0.45, the stress rises again, and then the stress decreases after reaching the second peak stress. It indicates that necking and fracture occur in the inner layers of TA1/AZ31B multi-layer composite during the compression processing. This phenomenon can be found in Fig.9.

Fig.9 illustrates the microstructure of TA1/AZ31B multi-layer composites after compression at 723 K with the strain rate 10 s^{-1}. Necking and fracture also occurs inTA1 layer in the middle of TA1/AZ31B multi-layer composite (Fig.9c, 9d), which is caused by the shearing and pressing stress, and the grain size is very fine (Fig.9f). The microstructure of TA1 layers on the outer side of TA1/AZ31B multi-layer composite has little change during the compression process and only has slight shearing deformation in the corner site. The deformed grain occurs along 45° shear direction (Fig.9a, 9e). AZ31B layer's grain microstructure is depicted in Fig.9d, 9b. The sample shows the deformed grain structures, which are characteristic for compressed material, as well as DRX fine grains around large deformation grain, indicating that the deformation is of inhomogeneity and asynchrony between TA1 and AZ31B during the compression processing.

Fig.10 illustrates the flow stress-strain curves of TA1, AZ31B, and TA1/AZ31B multi-layer composite in the temperature range of 573~723 K with the strain rate 1.0 s^{-1}. Through comparing the flow stress curves of TA1, AZ31B and TA1/AZ31B multi-layer composite, the flow stress curves of TA1/AZ31B multi-layer composite is between those of TA1 and AZ31B, and closes to that of AZ31B. It indicates that both TA1 and AZ31B have been deformed during the compression bonding process, but the deformation does not occur at the same time and is not uniform. The deformation of AZ31B is larger than that of TA1, and dynamic recrystallization occurs in AZ31B during the deformation processing. Therefore, TA1/AZ31B multi-layer composite is affected by deformation reduction, deformation temperature, strain rate, initial thickness of TA1 and AZ31B sheet, and other factors in the compression bonding process. The same phenomenon occurs during roll bonding process[5-7].

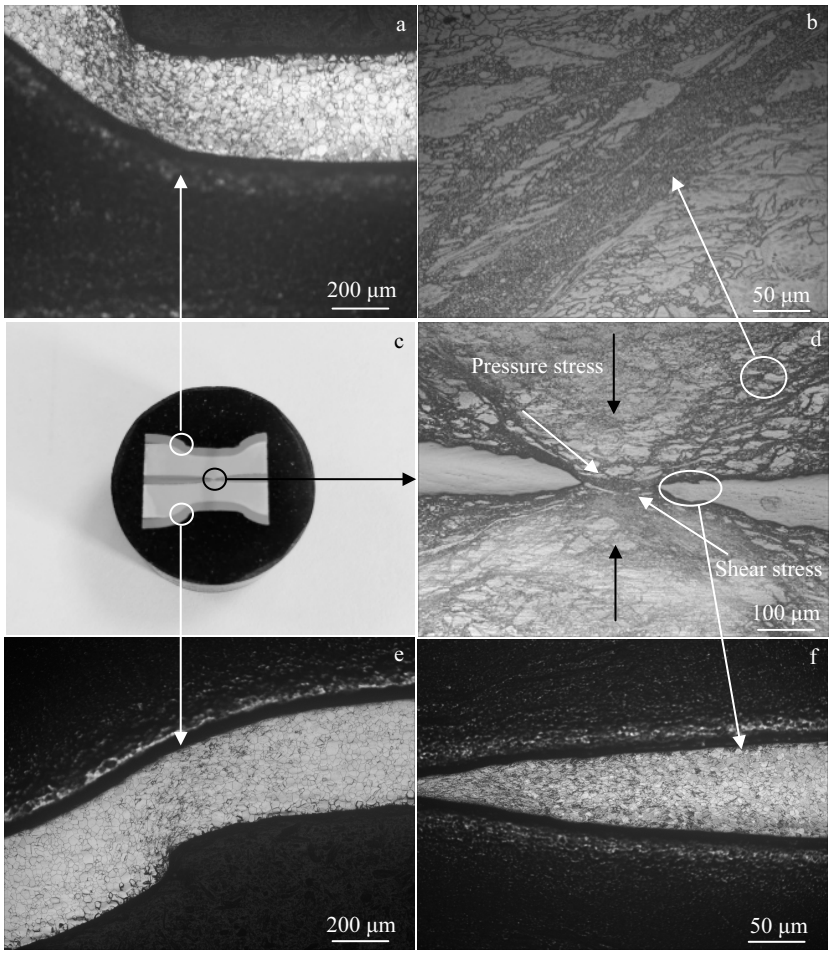

Fig.9 Microstructures of TA1/AZ31B multi-layer composites after compression at 723 K with the strain rate 10 s^{-1}

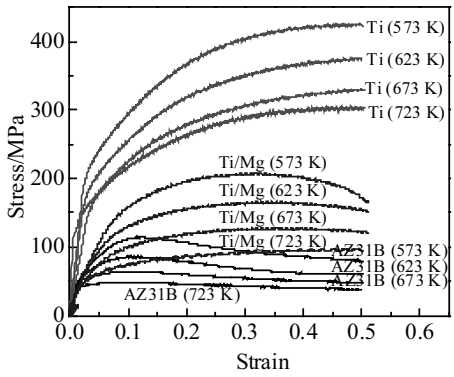

Fig.10 Flow stress-strain curves of the TA1, AZ31B and TA1/AZ31B multi-layer composites at $\dot{\varepsilon}$ =1.0 s^{-1}

2.3 Constitutive equations

It has been pointed out that the deformation process of the metal materials actually is very complicated. To explore the deformation of the TA1/AZ31B multi-layer composite, it is suggested to apply the constitutive equations to explore the relationship of the strain rate and the flow stress over the deformation temperature[15]. The influence of the strain rate and temperature on the deformation behaviors can be featured through the Zener-Hollomon parameter in an exponential equation as follows[16]:

$$Z = \dot{\varepsilon}\exp(\frac{Q}{RT}) \tag{1}$$

$$\dot{\varepsilon} = AF(\sigma)\exp(-\frac{Q}{RT}) \tag{2}$$

$$F(\sigma) = \begin{cases} \sigma^{n'} & \alpha\sigma < 0.8 \\ \exp(\beta\sigma) & \alpha\sigma > 1.2 \\ [\sinh(\alpha\sigma)]^n & \text{for all } \sigma \end{cases} \tag{3}$$

where $\dot{\varepsilon}$ refers to the strain rate; σ means the flow stress; A refers to the frequency factor; Q is apparent activation energy of composites deformation; gas constant is represented by R, defined as 8.314 J /mol·K; T stands for temperature in Kelvin, and n', β, α and n are the material constants.

The material constants have been determined through the flow stress data of the isothermal compression experiment under different processing conditions by the Arrhenius-type constitutive model. In the present research, the true strain of 0.1 has been viewed as a kind of examples to depict the solution procedures for the TA1/AZ31B multi-layer composite materials constants. Afterwards, the Z and $F(\sigma)$ were substituted into Eq. (2), which can result in

$$\dot{\varepsilon} = B\sigma^{n'} \tag{4}$$

$$\dot{\varepsilon} = C\exp(B\sigma) \tag{5}$$

where B and C refer to the material constants, both of which remain independent of the deformation temperature. Then, both sides taking logarithms of Eq.(4) and (5) have been considered and the equations below can be acquired:

$$\ln\sigma = \frac{1}{n'}\ln\dot{\varepsilon} - \frac{1}{n'}\ln B \tag{6}$$

$$\sigma = \frac{1}{\beta}\ln\dot{\varepsilon} - \frac{1}{\beta}\ln C \tag{7}$$

The slope of the lines in $\ln\sigma$ - $\ln\dot{\varepsilon}$ plot and the σ - $\ln\dot{\varepsilon}$ plot can be used to obtain the values of n' and β, as shown in Fig.11. Afterwards, it can obtain the relative value of $\alpha = \beta/n'$.

When it comes to the low stress levels, Eq. (2) can be expressed as below:

$$\dot{\varepsilon} = A[\sinh(\alpha\sigma)]^n \exp(-\frac{Q}{RT}) \tag{8}$$

When both sides taking natural logarithm of Eq. (8), have been considered, it would result in:

$$\ln[\sinh(\alpha\sigma)] = \frac{\ln\dot{\varepsilon}}{n} + \frac{Q}{nRT} - \frac{\ln A}{n} \tag{9}$$

For a specific temperature, Eq. (9) can be differentiated as:

$$\frac{\mathrm{d}\{\ln[\sinh(\alpha\sigma)]\}}{\mathrm{d}(\ln\dot{\varepsilon})} = \frac{1}{n} \tag{10}$$

The slopes of the lines of $\ln[\sinh(\alpha\sigma)]$ - $\ln\dot{\varepsilon}$ can be used for the calculation of the value of n, as presented in Fig.12a.

Based on Eq.(9), Q value under a specific strain rate could be acquired as what is listed below:

$$Q = Rn\frac{\mathrm{d}\{\ln[\sinh(\alpha\sigma)]\}}{\mathrm{d}(\frac{1}{T})} \tag{11}$$

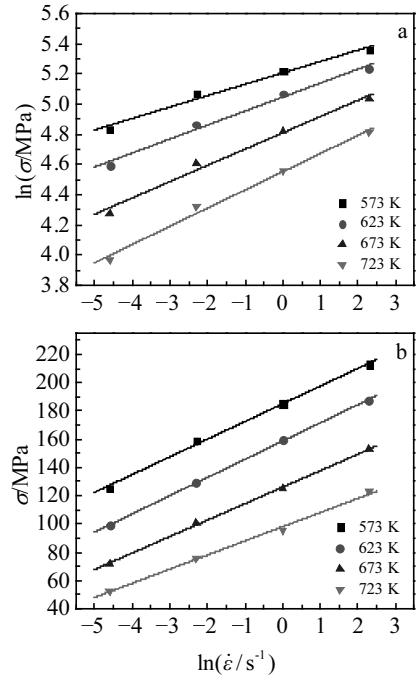

Fig.11 Relationship curves between $\ln\sigma$ and $\ln\dot{\varepsilon}$ (a); σ and $\ln\dot{\varepsilon}$ (b) for TA1/AZ31B multi-layer composite at true strain of 0.1

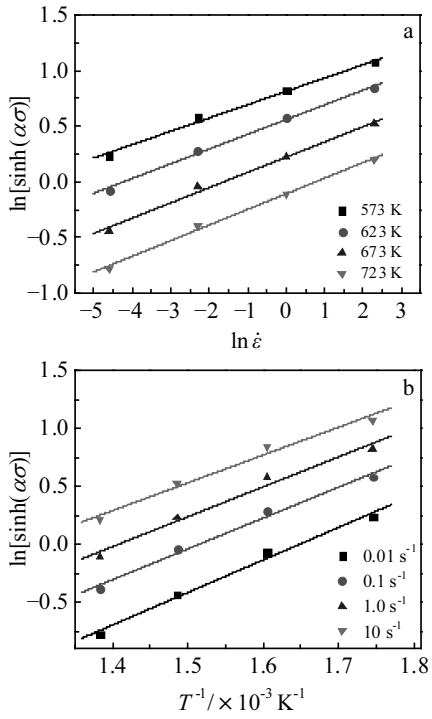

Fig.12 Relationship curves between $\ln[\sinh(\alpha\sigma)]$ and $\ln\dot{\varepsilon}$ (a); $\ln[\sinh(\alpha\sigma)]$ and T^{-1} (b) for TA1/AZ31B multi-layer composites at true strain of 0.1

The value of Q can be derived from the slopes in the plot of $\ln[\sinh(\alpha\sigma)]$-T^{-1}, as depicted in Fig.12b. Averaging the values of Q in different strain rates can determine its value. Value of A under a specific strain rate can be obtained from the intercept of the $\ln[\sinh(\alpha\sigma)]$-$\ln\dot{\varepsilon}$ plot.

When there are evaluations of the material constants, the flow stress in a specific strain can be forecast through the equation below:

$$\sigma=\frac{1}{\alpha}\ln\left\{\left(\frac{Z}{A}\right)^{\frac{1}{n}}+\left[\left(\frac{Z}{A}\right)^{\frac{2}{n}}+1\right]^{\frac{1}{2}}\right\} \tag{12}$$

Adopting this method, it can be calculated for the measurement of constitutive equations regarding TA1/AZ31B multi-layer composites having height reduction of 40%. The material constants of the Arrhenius model of the TA1/AZ31B multi-layer composites are listed in Table 3.

Afterwards, Eq. (12) can be used to obtain the Arrhenius-type model for TA1/AZ31B multi-layer composites.

The predicted value through the Arrhenius-type constitutive equation and the experimental value are compared under different processing situations in Fig.13.

The accuracy of the depicted models were tested through the standard statistical variables, for example the correlation coefficient (R) and average absolute relative error (AARE). R is regarded as the strength of linear correlation between the predicted and experimental which is listed below[17]:

Table 3 Constitutive equation parameters at different true strains for height reduction of 40%

ε	ln$A$	α	n	Q/J·(mol·K)$^{-1}$
0.05	25.108 8	0.011 1	9.128 1	151.085 0
0.10	30.469 1	0.008 3	8.061 4	178.842
0.15	32.974 5	0.007 4	8.073 0	192.393 5
0.20	34.084 2	0.007 0	8.054 7	198.417 3
0.25	34.135 2	0.006 7	8.020 7	198.345 2
0.30	32.320 5	0.006 6	7.822 1	188.444 5
0.35	32.343 8	0.006 5	8.028 2	188.475 5
0.40	35.088 9	0.006 7	9.029 7	204.983 6
0.45	40.002 9	0.007 2	10.884 1	234.750 1

$$R=\frac{\sum_{i=1}^{N}(E_i-\bar{E})(P_i-\bar{P})}{\sqrt{\sum_{i=1}^{N}(E_i-\bar{E})^2\sum_{i=1}^{N}(P_i-\bar{P})^2}} \tag{13}$$

where P and E refer to the predicted and the experimental flow stress (MPa) based on developed constitutive equation, respectively; The mean values of E and P are $\bar{E}$ and $\bar{P}$, respectively. N is the total number of data adopted in this study.

A statistical analysis was conducted based on Arrhenius-type constitutive model. Predictions were made through the comparison with the relative experimental statistics, and then the average absolute relative error (AARE) can be expressed as[18]:

$$\mathrm{AARE}=\frac{1}{N}\sum_{i=1}^{N}\left|\frac{E_i-P_i}{E_i}\right|\times 100\% \tag{14}$$

Fig.14 demonstrates the good agreement between the predicted value and experimental value. The R value for the Arrhenius type model is calculated to be 0.991 while AARE value is calculated to be 3.976%, demonstrating that the model can accurately forecast the flow stress under deformation situations. These results demonstrate the good forecasting ability of this constitutive equation to TA1/AZ31B multi-layer composites.

2.4 Processing maps

On the basis of the principles of dynamic material model (DMM), the processing map is given. It is overlapped with the dissipation of the power provided by a specific source. It is frequently applied for the evaluation of the material workability, serving as a kind of function of process parameters, such as strain, strain rate and temperature[19-22]. Under the DMM model, the workpiece in the hot deformation is regarded as the dissipater of power. The features of power dissipation can be obtained via the microstructural changes, which are demonstrated and calculated regarding the power dissipation efficiency by

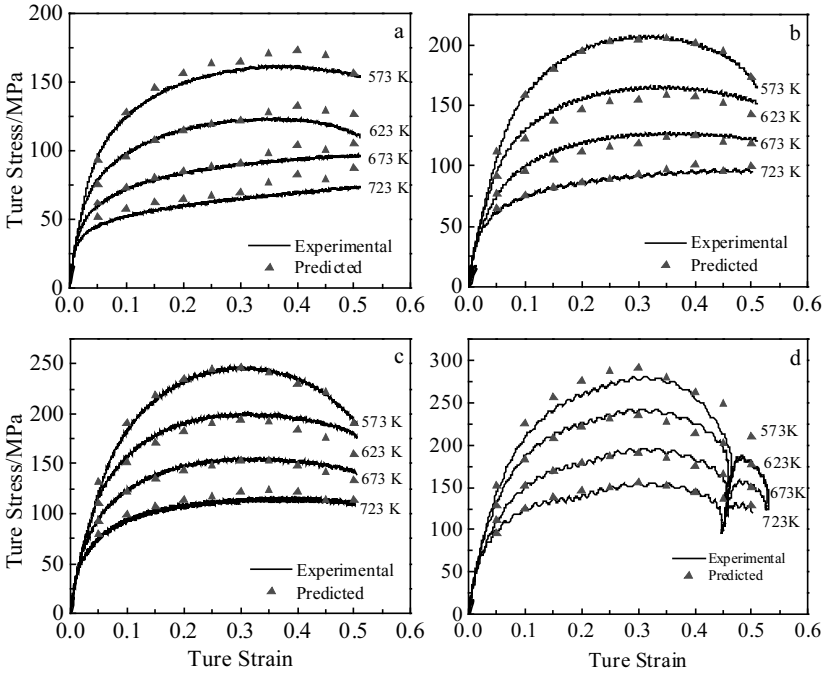

Fig.13 Comparison between the experiment and predicted flow stress at the $\dot{\varepsilon}$ of 0.01 s^{-1} (a), 0.1 s^{-1} (b), 1.0 s^{-1} (c), and 10 s^{-1} (d)

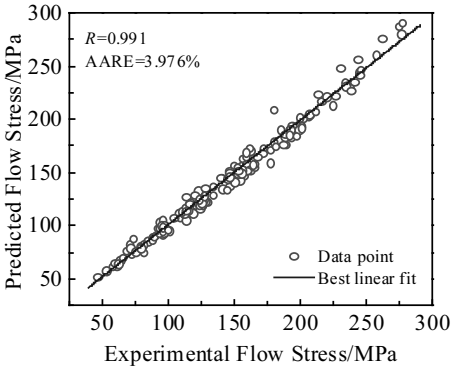

Fig.14 Correlation between the experimental and predicted flow stress values from the Arrhenius-type model (height reduction of 40%)

$$\eta = \frac{2m}{m+1} \tag{15}$$

in which, m refers to strain rate sensitivity parameter and has been figured up as a function of $\dot{\varepsilon}$. $\ln\sigma$ versus $\ln\dot{\varepsilon}$ curve has been fitted by a cubic spline:

$$m = \frac{\partial(\ln\sigma)}{\partial(\ln\dot{\varepsilon})} \tag{16}$$

The variation of η with temperature and strain rates composes the processing map, demonstrating multiple domains, which can be related with particular microstructural mechanisms. As what is known to all, there is deformed instability in multi-layer composite in the plastic deformation phase. The continuum instability criterion of irreversible thermodynamics was used to identify the regimes of flow instability. Kalyan[23] proposed the instability conditions as:

$$\xi(\dot{\varepsilon}) = \frac{\partial \ln[\frac{m}{m+1}]}{\partial \ln \dot{\varepsilon}} + m < 0 \tag{17}$$

It has been used for the description of the temperature-strain rate mechanisms of flow instability over the processing map. A cubic spline function has been used in the plot of $\ln\sigma$ versus $\ln\dot{\varepsilon}$, and the strain rate sensitivity (m) has been assessed serving as strain rate's function. This has been repeated at different temperatures. The power dissipation's efficiency and dimensionless instability parameter have been calculated based on a set of m-values to acquire the power dissipation map. Finally, the processing maps have been acquired through superimposing the instability map over the power dissipation map.

Fig.15 demonstrates the construction of processing map of TA1/AZ31B multi-layer composites at the temperatures between 573 K and 723 K, strain rates from 0.01~10 s^{-1}. The processing map of TA1/AZ31B multi-layer composites has one instability domain. It is in the deformation temperature scale between 573 and 692 K while the strain rate is between 0.6 and 10 s^{-1}. There is a gradual decrease of power dissipation efficiency with the increase of the strain rate and reduction in temperature within this domain. It implies that the composites' workability is worse through the increase of strain rate and decrease of temperature. Such characteristic has been

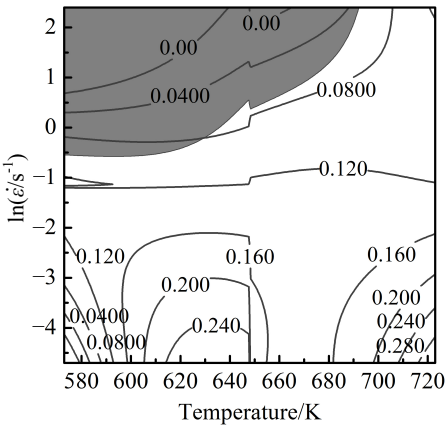

Fig.15 Processing map of TA1/AZ31B multi-layer composite obtained at true strain of 0.5

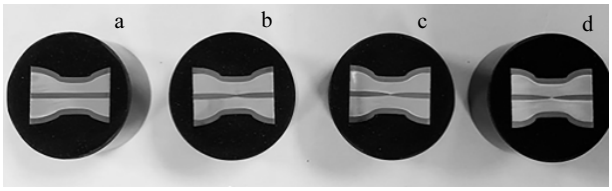

Fig.16 Macro pictures of TA1/AZ31B multi-layer composites at the strains rates of $\dot{\varepsilon}$=0.01 s^{-1} (a), $\dot{\varepsilon}$=0.1 s^{-1} (b), $\dot{\varepsilon}$=1.0 s^{-1} (c), and $\dot{\varepsilon}$=10 s^{-1} (d) at 723 K

found to be classical in a fracture process in Fig.9. The deformation of specimens' middle layer occurs under such situations, which demonstrates fracture along the maximum shear stress planes. The optimum parameter has been determined to be the temperature of 723 K and the strain rate of 0.01 s^{-1} with power dissipation's maximum efficiency of 28%.

Fig.16 demonstrates the specimen's macroscopic structure of TA1/AZ31B multi-layer composite at 723 K and the strain rates of 0.01~10 s^{-1}. Good bonding is presented by the interface of TA1/AZ31B multi-layer composites of 723 K with 0.01 s^{-1} (as shown in Fig.16a). With the increase of the strain rate, there is necking and fracture occurring in the middle TA1-layer (as shown in Fig.16b, 16c, and 16d). Thus, it has been shown that the calculation results of the processing map can be applied for the TA1/AZ31B multi-layer composite.

3 Conclusions

1) TA1/AZ31B multi-layer composite has positive strain rate sensitivity. When the strain rate is larger and the deformation temperature is lower, it is more difficult to achieve steady deformation. During the compression bonding process, dynamic recrystallization (DRX) occurs in AZ31B layer of TA1/AZ31B multi-layer composite. With the increase of deformation temperatures from 573 K to 723 K the average peak stress of TA1/AZ31B multi-layer composite decreases by 113 MPa.

2) The Arrhenius-type model can be used for the numerical simulation of hot working of TA1/AZ31B multi-layer composite , which adopts the Arrhenius constitutive model constructed by the constitutive equation of TA1/AZ31B multi-layer composite in the temperature range of 573~723 K and the strain rate range of 0.01~10 s^{-1}. The value of R for the Arrhenius-type model is 0.991 and the value of AARE is 3.976%.

3) There is one instability domain in the processing map of isothermal compression of TA1/AZ31B multi-layer composite. It is in the deformation temperature range from 573 K to 692 K and the strain rate range from 0.6 s^{-1} to 10 s^{-1}. The optimum processing parameters of TA1/AZ31B multi-layer composite are the temperature 723 K and the strain rate 0.01 s^{-1} with the maximum efficiency of power dissipation of 28%.

References

1 Chaudharig P, Acoff V. *Composites Science & Technology*[J], 2009, 69(10): 1667
2 Abbasi M, Toroghinejad M R. *Journal of Materials Processing Technology*[J], 2010, 210(3): 560
3 Movahedi M, Madaah H R, Kokabi A H. *Materials Science & Engineering A*[J], 2008, 487(1): 417
4 Jamaatir, Toroghinejad M R. *Materials Science & Engineering A*[J], 2010, 527(9): 2320
5 Li Xiaobing, Zu Guoyin, Wang Ping. *Materials Science & Engineering A*[J], 2013, 575(13): 61
6 Li Xiaobing, Zu Guoyin, Wang Ping. *Transactions of Nonferrous Metals Society of China*[J], 2015, 25(1): 36
7 Kim Jungsu, Lee Kwangseok, Yong Namkwon *et al. Materials Science & Engineering A*[J], 2015, 628: 1
8 Luo Jianguo, Acoff V L. *Materials Science & Engineering A*[J], 2004, 379(1): 164
9 Wang Tao, Cao Rui, Chen Jianhong *et al. Journal of Mechanical Engineering*[J], 2014, 50(4): 75
10 Sun J, Tong W P, Zou L *et al*. *Materials & Design*[J], 2013, 47(9): 408
11 Yasser F. *Alexandria Engineering Journal*[J], 2014, 53(2): 289
12 Wu Jiaqi, Wang Wenxian, Cao Xiaoqing *et al. Rare Metal Materials & Engineering*[J], 2017, 46(3): 640
13 Motevalli P D, Eghbalib B. *Materials Science and Engineering A*[J], 2015, 628 (3): 135
14 Ezatpour H R, Sajjad S A, Sabzevar M H *et al. Transactions of Nonferrous Metals Society of China*[J], 2017, 27(6): 1248
15 Luan Baifeng, Qiu Risheng, Li Chunhong *et al. Transactions of Nonferrous Metals Society of China*[J], 2015, 25(4): 1056
16 Cai Jun, Wang Kuaishe, Han Yingying. *High Temperature Materials and Processes*[J], 2016, 35(3): 297
17 Li Jiang, Li Fuguo, Cai Jun *et al. Computational Materials Science*[J], 2013, 71(3): 56

18 Hong Ying, Feng Xiaofeng, Wei Dongdong *et al. Materials Science and Engineering A*[J], 2012, 536(1): 216
19 Fan J K, Kou H C, Lai M J *et al. Materials & Design*[J], 2013, 49: 945
20 Quan Guozheng, Wang Yang, Yu Chuntang *et al. Materials Science and Engineering A*[J], 2013, 564:46
21 Zhang Tian, Tao Yourui, Wang Xueyin. *Transactions of Nonferrous Metals Society of China*[J], 2014, 24(5): 1337
22 Hao Shiming, Xie Jingpei, Wang Aiqin *et al. Transactions of Nonferrous Metals Society of China*[J], 2014, 24(8): 2468
23 Zhou Ge, Ding Hua, Cao Furong *et al. Transactions of Nonferrous Metals Society of China*[J], 2012, 22(7): 1575

TA1/AZ31B 多层复合材料在等温压缩过程中的变形行为

张 兵[1,2,3]，姚 苏[1,3]，王秋雨[1,3]，李 娟[2]，张 东[2]，赵田丽[1,2]，王 文[1,2]，蔡 军[1,2]，王快社[1,2]

(1. 西安建筑科技大学，陕西 西安 710055)

(2. 金川集团有限公司 镍钴资源综合利用国家重点实验室，甘肃 金昌 737100)

(3. 功能材料加工国家地方联合工程研究中心，陕西 西安 710055)

摘 要：采用等温压缩实验研究了在变形温度为 573~723 K，应变速率范围为 0.01~10 s^{-1}，压下量 30%~50%的条件下 TA1/AZ31B 多层复合材料的塑性变形行为并利用光学显微镜观察显微组织的变化。研究表明：TA1 和 AZ31B 在压缩复合过程中均发生塑性变形，但是钛/镁多层复合材料各层的变形不同时且不均匀，AZ31B 层的变形程度大于 TA1 层，且在变形过程中 AZ31B 层发生了动态再结晶。当应变速率为 10 s^{-1} 时，中间 TA1 层出现颈缩和断裂。计算结果证明，Arrhenius 本构方程可以准确预测 TA1/AZ31B 多层复合材料的流动应力行为，其平均绝对相对误差为 3.976%，相关系数为 0.991。此外，基于动态材料模型(DMM)理论建立了 TA1/AZ31B 多层复合材料在真应变为 0.5 下的加工图，确定最佳加工条件为 723 K 温度下，应变速率为 0.01 s^{-1}，此时最大功率耗散值为 28%。同时，TA1/AZ31B 多层复合材料的加工图中存在一个不稳定区域，即变形温度范围为 573~ 692 K 时应变速率范围为 0.6~10 s^{-1}。

关键词：TA1/AZ31B 多层复合材料；等温压缩；变形行为；本构方程；加工图

作者简介：张 兵，男，1969 年生，博士，教授，西安建筑科技大学冶金工程学院，陕西 西安 710055，电话：029-82202931，E-mail: r.zhang1112@163.com